Point-spread function and photon transfer of a CCD for space-based astronomy

Conference or Workshop Item

Point-spread function and photon transfer of a CCD for space-based astronomy

Edgar A. H. Allanwood[a], Neil J. Murray[a], Konstantin D. Stefanov[a], David J. Burt[b], Andrew D. Holland[a]

[a]Centre for Electronic Imaging, The Open University, Milton Keynes, MK7 6AA, UK;
[b]e2v technologies plc, 106 Waterhouse Lane, Chelmsford, CM1 2QU, UK

ABSTRACT

A front-illuminated development Euclid charge-coupled device (CCD) is tested to observe the CCD point-spread function (PSF) relative to signal size using a single-pixel photon transfer curve (SP-PTC) technique. In the process of generating a SP-PTC charge redistribution effects were observed. In attempting to show that charge redistribution can be caused by exposing a charge-populated well in the CCD array to further illumination, excess charge became apparent in recorded data. Excess charge is suggested to be proportionally generated in the CCD array if existing charge is subjected to further illumination before transfer and readout. The construction of an optical test bench and CCD operating variables are discussed alongside systematic error concerns and mitigation techniques.

Keywords: CCD, PSF, PTC, spot projection, Euclid, charge redistribution

1. INTRODUCTION

1.1 Euclid and the Dark Universe

Weak gravitational lensing (WGL) surveys are increasing in popularity and requirements for how thoroughly camera systems are understood are becoming more stringent. This paper focuses on experiments carried out on a CCD developed for the European Space Agency (ESA) Euclid mission. Euclid will attempt to indirectly observe the gravitational distribution of the dark universe and will operate two main instruments:[1] the Visible Imager (VIS) and Near-Infrared Spectrometer-Photometer (NISP) to measure the shape and spectra of observed galaxies respectively. The evolution of the VIS point-spread function (PSF) during the mission lifetime is essential knowledge as it is required to process returned images into useful data, on which shape measurements can be performed for WGL.

A photon transfer curve (PTC) provides an estimation of CCD gain and linearity, however; the mean-variance of 'thick' red-enhanced devices has been shown[2] to be increasingly non-linear as signal increases, with greater non-linearity in 'thicker' devices. A charge redistribution mechanism between pixels has been suggested as the culprit. This study focuses on the radiation damage free (control region) performance of a CCD subjected to spot and flat-field illuminations, using traditional photon transfer techniques and signal-relative shape based measurements. Furthermore, the influence of pre-existing pixel charge on the distribution of subsequent photo-generated charge is investigated experimentally.

1.2 The Device Under Test

The device under test (DUT) is a pre-development and front-illuminated e2v CCD273. Using a thin-gate deep depletion configuration, the sensor is designed for improved red and near infra-red (NIR) response. The n-channel device utilises 12 μm square pixels and is mapped into four 2×2 kpixel quadrants (two halves, four nodes) with a four-phase electrode configuration and central charge injection structure. More information on the development of the CCD273 including a detailed floor plan of the device can be found in SPIE proceedings[3] by J. Endicott (2012).

edgar.allanwood@open.ac.uk; www.open.ac.uk/cei

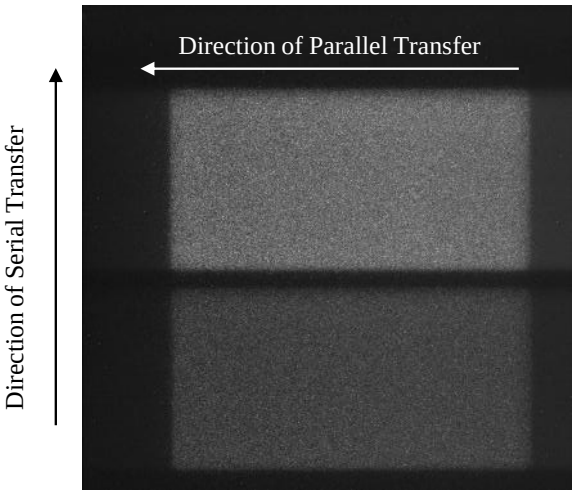

Figure 1. Node A1 of the CCD273 after 2000 trap pumps during device cooling. The brigher rectangle indicates the area of EOL proton fluence whilst the darker rectangle represents an area of EOL/2 fluence. Experiments were conducted in the control region towards the top-left of the image, close to the read-out node.

In this document unless stated otherwise a 200 kpix.s^{-1} readout rate is used with a $2-2-2-2$ coincident parallel clocking sequence and 10 V image clocks. $2-2-2-2$ clocking is used primarily to improve CTE such that any trapped charge is more likely to be emitted back into the packet in which it originated.[4] The optimum full-well capacity improves due to charge packets never having less than two barrier phases as with $2-3-2$ charge transfer. The image clock voltage was selected based on data[5] which demonstrates the mean variance differences between $2-3-2$ and $2-2-2$ clocking on the n-channel e2v CCD204: a structurally similar device.

Sections of the DUT were irradiated[6] selectively at Kernfysisch Versneller Institut with 50MeV protons, resulting in a 10MeV equivalent end of life (EOL) proton fluence of 4.8×10^9 protons.cm^{-2}. Irradiated regions of the device were chosen in such a way that radiation-free control regions were plentiful to allow for geometrical calculations based on spot measurements to be performed in different areas. This paper will focus on the device behaviour in a non-irradiated control region, shown in Figure 1.

2. OPTICAL TEST BENCH

2.1 Construction

An optical test bench was assembled with the intent of projecting spots and uniform illuminations onto the DUT which is positioned behind the window of a vacuum chamber. The DUT is cooled by a CryoTiger with the CCD positioned on a copper cold bench, coupled by copper braids to the cold finger at the rear of the chamber (Figure 2). A pair of PT100 resistive temperature sensors monitor the device temperature which is approximately $-110\,^{\circ}$C for all experiments. Prior to cooling the chamber is pumped down to 1.6×10^{-6} mbar.

The spot projection system is constructed from a Thorlabs SM1 lens tube system and is translated parallel (XY) to the CCD focal plane by two Newport ILS100-M translation stages. The system is focused by a LTA-HS translation stage axis mounted at normal (Z) to the XY-plane. The entire system is enclosed in a dark box constructed from high density foam core board and black anodised aluminium extrusions. The optics (Figure 3) consist of an achromatic pair which image an LED-illuminated 5 μm pinhole. The system was commissioned using a CMOS camera with 5.8 μm pixels (approximately half the size of the CCD273 pixels) to achieve a sharp focus at a known distance, thus allowing the optimum focus to be found algorithmically *in situ* when using the CCD and translation stages. The full-width half-maximum of the spot, measured by a Gaussian fit is consistently between 9 μm and 10 μm, a consequence of the diffraction limit of the achromatic lenses. The flat field illumination system sits parallel to the spot projection optics and uses an SM1 engineered diffuser achieving uniformity of < 5 ke^- at $100ke$ across the region of interest used for these experiments.

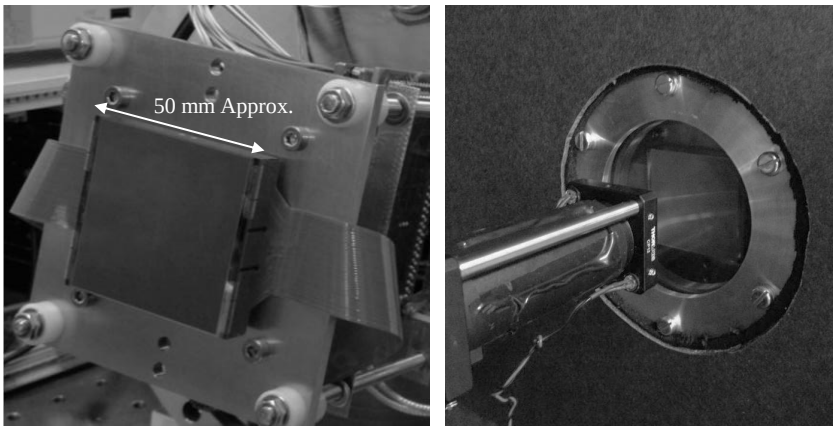

Figure 2. Left: Device shown mounted on copper cold bench with flexi routed behind to camera electronics which are supported on M4 studs protruding from the chamber rear. Right: The positioning of the device relative to the vacuum chamber window. A 1 mm gap was left between the CCD surface and the glass prior to pumping down the chamber. The device was not mounted normal to the optical axis due to mechanical limitations in the mounting technique.

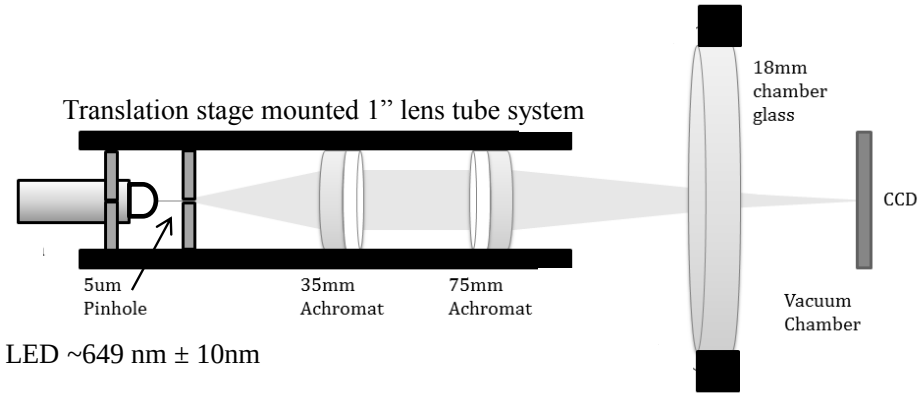

Figure 3. A simplified diagram of spot projection optics.

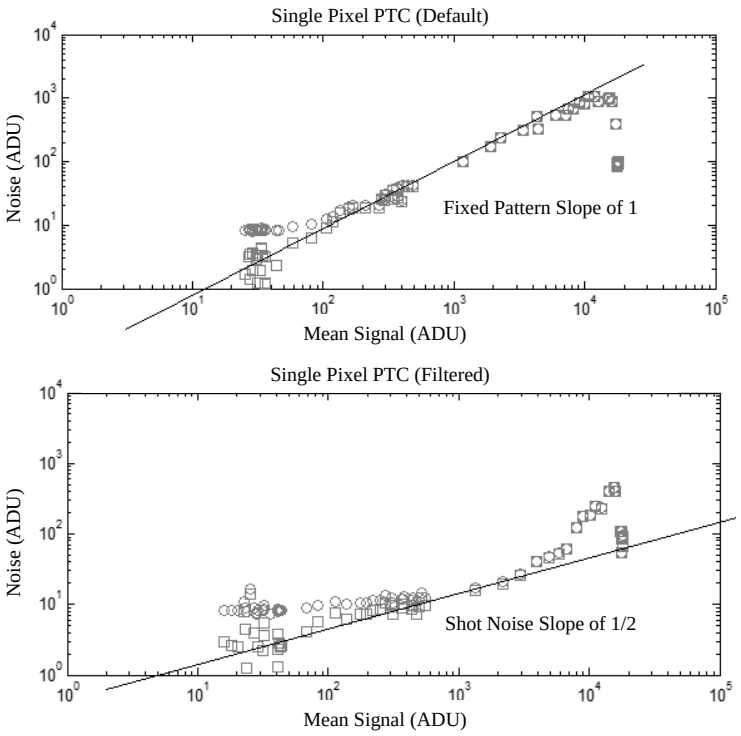

Figure 4. Two SP-PTCs showing noise and read-noise subtracted curves generated from the same dataset. The lower SP-PTC has the centre of mass filter applied to remove smearing from the mean spot image; a consequence of system vibrations. These plots show that vibration causes a dominant noise component. The deviation from the shot-noise limited slope of a half in the lower image shows the reduced efficacy of filtered data at high signal values. Whilst the SP-PTC does not provide useful responsivity data it indicates the signal levels at which the shape of the spot is potentially changing the noise performance.

2.2 Single Pixel Photon Transfer Curve (SP-PTC)

Prior to any spot-based measurements the spot is focused and centred. Firstly, using a centre of mass algorithm the 3×3 pixel grid which the spot occupies is evaluated. The centre of mass is calculated and converted into microns in order to physically correct the spot position should it be off-centre. This process is run recursively until the spot is centred to a satisfactory percentage (2% in both axes).

Generating a SP-PTC in the presence of mechanical vibration produced a fixed-pattern limited characteristic as in Figure 4. This systematic error proved problematic as it blurred the PSF, as is the nature of generating the mean image from an array of spot images where the spot varies in location. As a solution the the mean signal values from only well-centred spots were used. In this case the SP-PTC characteristic follows a shot-noise limited regime up until the blooming threshold of the device at which point the vertical spreading of charge compromises the centroid criterion until no images are accepted to generate a mean. This shows that vibration noise can be eliminated by filtering to restore the shot noise slope. The plot does not corroborate the conversion gain returned by a flat-field PTC, however; the charge collection behaviour is the main motivation for gathering the data. Using a spot-plot (Figure 5), the average image of each PTC light level can be plotted in sequence for both centroided and non-centroided SP-PTCs. Furthermore a directional measure of charge spread, aspect ratio (AR), can be extracted by comparing the amount of signal across the spot in the column and row direction. It was observed that as signal increases the spot appears widen in the row direction at 100 $k\mathrm{e}^-$ prior to blooming at the full well capacity of 250 $k\mathrm{e}^-$, prompting a further study of charge collection behaviour.

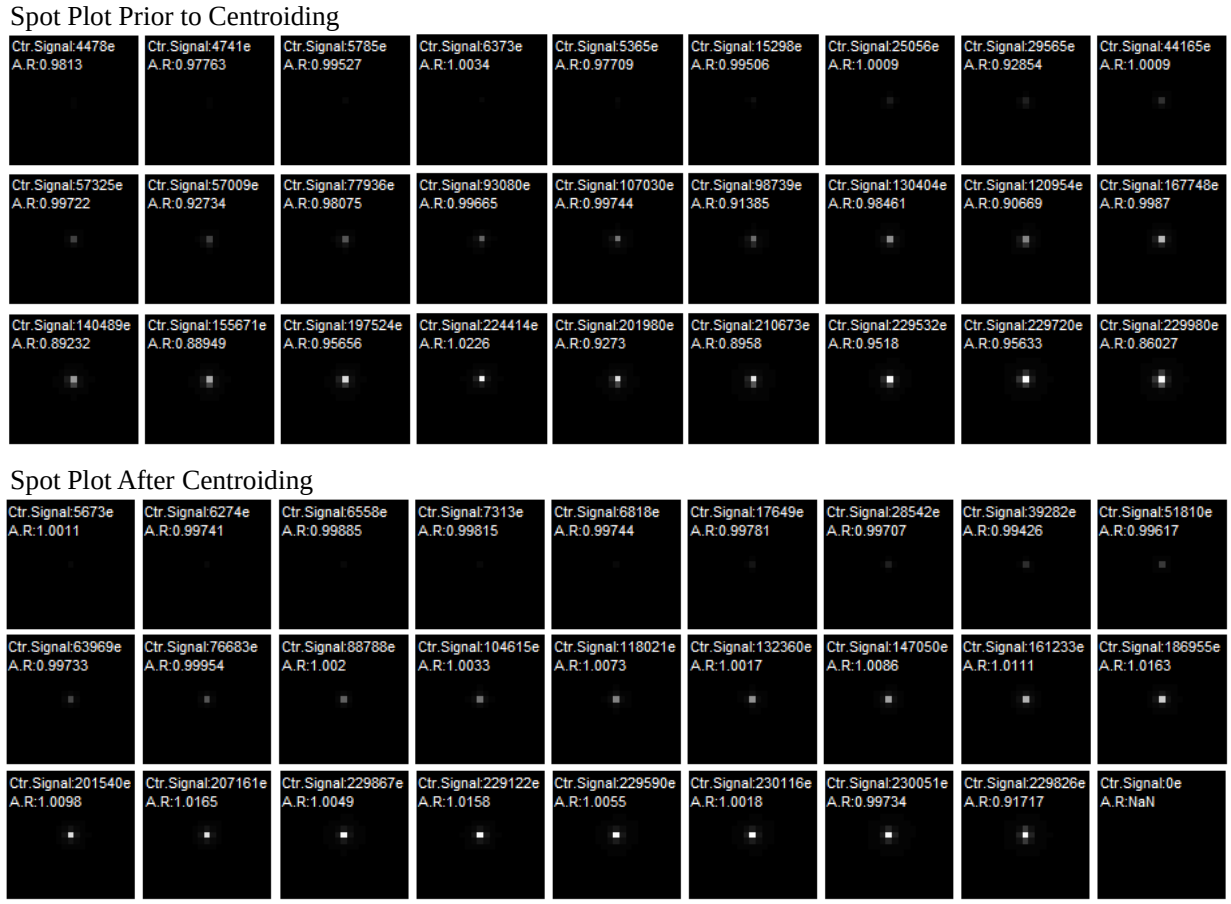

Figure 5. Two spot-plots generated from the same set of SP-PTC data. The centroiding algorithm generates average images from well-centred spots only allowing charge spreading behaviour with respect to signal to be better observed.

3. CHARGE DISTRIBUTION

In the previous section the filtered PTC inferred that as spot illumination is increased in brightness, the shape of the PSF changes with separate components: At first the charge spread laterally before spreading vertically as with blooming seen in all devices. This led to an investigation to find out why charge spreads with this behaviour. Many postulations were made, however; the most cogent idea suggested that the more charge there is in a potential well, the less chance there is of a photo-electron finding that potential well compared to neighbouring pixels. In response, a proof-of concept test was arranged.

3.1 Flat Illumination Following Line

A flat illumination followed by a dumped forward parallel transfer of 2065 rows and a backward parallel transfer of 1030 rows was the method used to insert a line of charge into the CCD. To test the existence of any redistributed charge the image consisting of the line only was read out and saved before being followed by image of the same nature with a subsequent LED flash applied to the array. Figure 6 shows the before and after appearance. Without looking at the numerics, this seemed visually confirmatory of the theory thus a further experiment was organised to investigate the charge redistribution theory.

3.2 Flat Illumination Following Spot

A spot was focused on to a radiation-free region of the DUT and a collection of images were generated as follows, each an average of 100 frames:

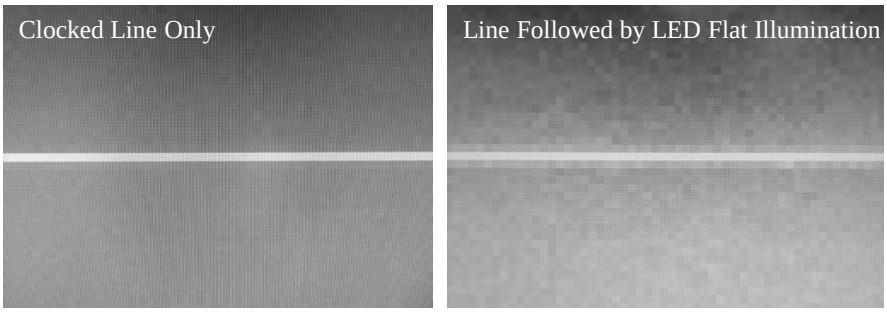

Figure 6. Left: A line clocked into a CCD via forward and back clocking a flat illumination. Right: The same process followed by an additional flat illumination prior to transfer and readout.

1. Control image (background only)
2. Spot only
3. Flat illumination only
4. Spot followed by a flat illumination.

The subtraction of mean image (2: Spot) from mean image (4: Spot + Flat), in an ideal device would result in image (3: Flat). Figure 7 shows an excess charge in the centre pixel visible as a peak in the difference profile. At first this seemed the result of an unknown systematic error as it contradicted the theory seemingly proven in the proof of concept experiment. The LED control waveforms were analysed for any discrepancies in current or timings using an oscilloscope, however; no errors were discovered. In an attempt to better understand this spurious excess charge generation a further experiment was proposed.

3.3 Spot Projected onto Clocked Line

In order to further examine the excess charge generation a spot of 35 $k\mathrm{e}^-$ was projected onto a line of varying intensity with the line being generated as in 3.1. Four sets of 100 images were collected and averaged as in Figure 8.

1. Control image (background only)
2. Spot only
3. Line only
4. Line followed by a spot illumination.

With an ideal device, mean image (4: Line + Spot) minus mean image (3: Line) would result in mean image (2: Spot). The values of the centre pixel for (2: Spot) and the subtraction image of (4) minus (3) are shown in Figure 9. The excess charge is defined as the difference between the spot only and the difference image spot, which in an ideal device would be zero. The top line in Figure 9 shows a linear increase in excess charge as the line signal on which the spot is projected is increased from 8 $k\mathrm{e}^-$ to 90 $k\mathrm{e}^-$ in 11 steps.

4. CONCLUSIONS

This paper describes the construction of an optical test bench and the steps taken to investigate the shape of the PSF with respect to signal level in un-irradiated operation. In the case of multiple light exposures excess charge appears to be generated by some unknown mechanism in this particular type of device - a front-illuminated, red-enhanced, development e2v CCD273. The observed excess charge is proportional to the amount of signal already stored in the array. When binning charges in the area immediately around the spot and line the

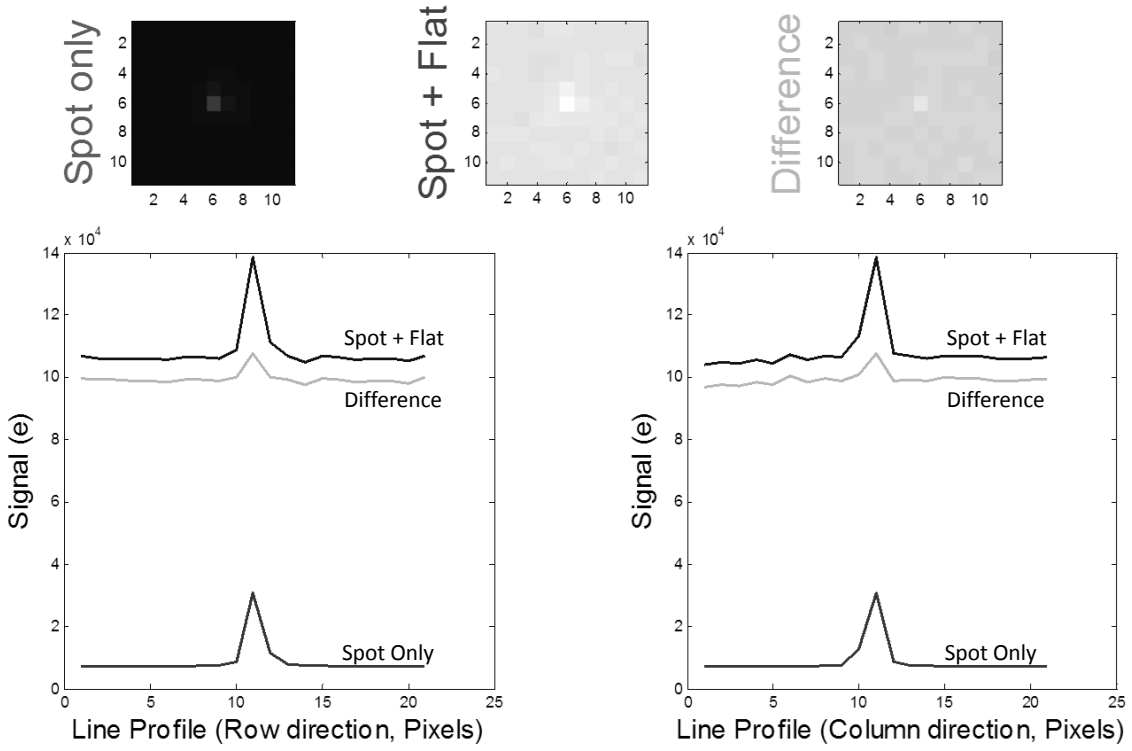

Figure 7. From this figure an excess charge of 4 ke^- is shown when a 100 ke^- flat illumination follows a 50 ke^- spot.

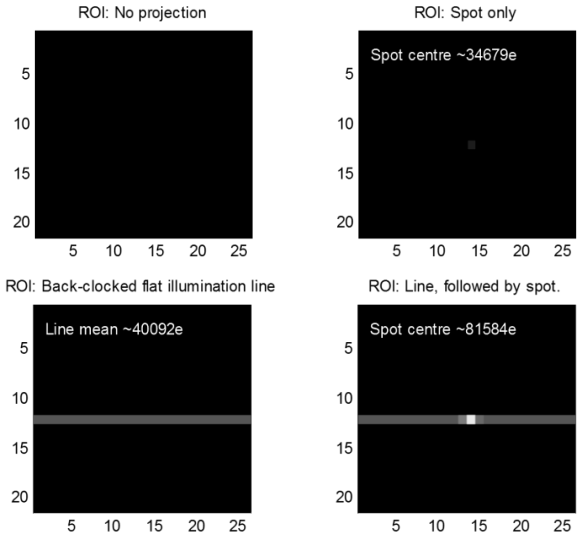

Figure 8. The four source images for the line, line-spot experiment: control (background), spot projection only, line projection only and line followed by spot. Each image represents an average of 100 images. At these particular levels of signal there is an excess charge in the centre pixel of 6.8 ke^-.

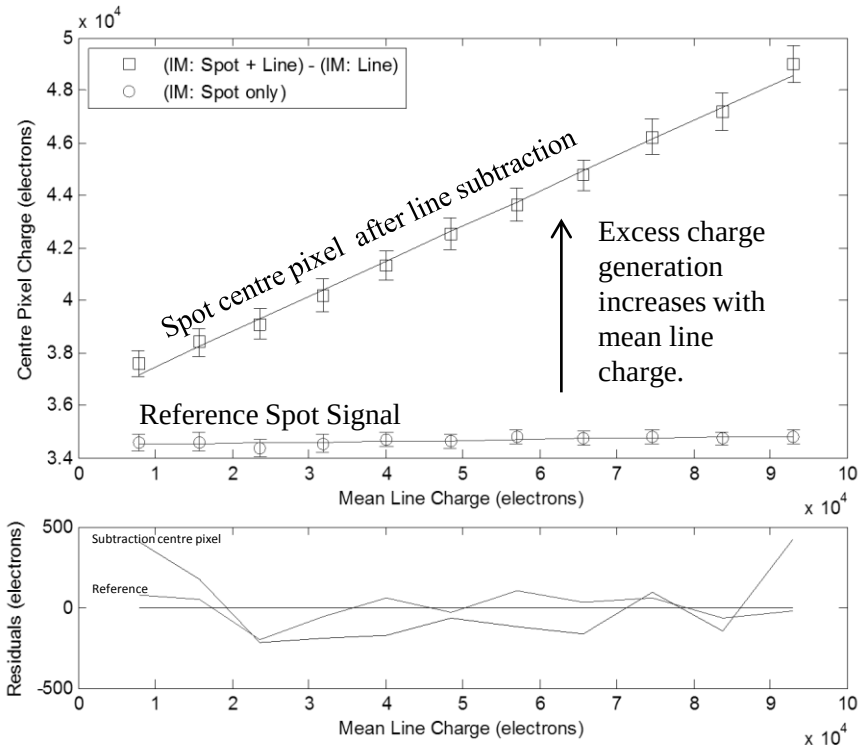

Figure 9. Excess charge with respect to mean line charge, with residuals. The magnitude of the noise in the subtraction is calculated from the standard deviations of the (IM: Spot + Line) and (IM: Line) added in quadrature.

percentage increase in charge is the same, thus it is an apparent excess charge generation effect and not charge redistribution. This was shown to be the case experimentally on two separate camera systems utilising the same sensor model and by two separate parties. The course of action will be to apply the same test to back-illuminated (BI) sensors to see if the same effect occurs. Asserting the wavelength dependence of the effect is also a priority. The linearity of the illumination appears to be linear therefore perhaps there could be some form of non-linear system gain with respect to signal, however this is unlikely.

From this work it is recommended that as many devices as possible are compared for their behaviour during the excess charge experiments. If the effect does not exhibit in back-illuminated sensors then they will be more preferable for optical characterisation than pre-development front-illuminated devices in future. These experiments are very much a work in progress - a mystery which will hopefully be understood in the following year.

REFERENCES

[1] Regregier, A., "Euclid imaging consortium science book," *arXiv* **1001.0061** (2010).

[2] Downing, M., "CCD riddle: a) signal vs time: linear; b) signal vs variance: non-linear," in [*High Energy, Optical and Infrared Detectors for Astronomy II*], Andrew D. Holland, D. A. D., ed., *Proc. SPIE* **6276** (2006).

[3] Endicott, J., "Charge-coupled devices for the ESA Euclid M-class mission," in [*High Energy, Optical and Infrared Detectors for Astronomy V*], Andrew D. Holland, J. W. B., ed., *Proc. SPIE* **8453** (2012).

[4] Murray, N. J., "Mitigating radiation-induced charge transfer inefficiency in full-frame CCD applications by 'pumping' traps," in [*High Energy, Optical and Infrared Detectors for Astronomy V*], Andrew D. Holland, J. W. B., ed., *Proc. SPIE* **8453** (2012).

[5] Clarke, A. S., [*Silvaco 3D Modelling of Device Structures and Model Verification on Custom-designed Test Structures*] (2013).

[6] Gow, J. P. D., "Assessment of proton radiation-induced charge transfer inefficiency in the CCD273 detector for the Euclid dark energy mission," in [*High Energy, Optical and Infrared Detectors for Astronomy V*], Andrew D. Holland, J. W. B., ed., *Proc. SPIE* **8453** (2012).